Molecular determinants of metazoan tricRNA biogenesis

Casey A. Schmidt[1,2], Joseph D. Giusto[3] and A. Gregory Matera[1,2,3,4,5,*]

[1] Integrative Program for Biological and Genome Sciences, University of North Carolina, Chapel Hill, NC, 27599, USA
[2] Curriculum in Genetics and Molecular Biology, University of North Carolina, Chapel Hill, NC, 27599, USA
[3] Department of Biology, University of North Carolina, Chapel Hill, NC, 27599, USA
[4] Department of Genetics, University of North Carolina, Chapel Hill, NC, 27599, USA
[5] Lineberger Comprehensive Cancer Center, University of North Carolina, Chapel Hill, NC, 27599, USA

* To whom correspondence should be addressed. Tel: +1 (919) 962-4567; Fax: +1 (919) 962-4574; Email: matera@unc.edu

ABSTRACT

Mature tRNAs are generated by multiple post-transcriptional processing steps, which can include intron removal. Recently, our laboratory discovered a new class of metazoan circular RNAs formed by ligation of excised tRNA introns; we termed these molecules tRNA intronic circular (tric)RNAs. To investigate the mechanism of tricRNA biogenesis, we generated constructs that replace the native introns of two *Drosophila* tRNA genes with the Broccoli fluorescent RNA aptamer. Using these reporters, we identified *cis*-acting elements required for tricRNA formation in both human and fly cells. We observed that disrupting the conserved anticodon-intron base pair dramatically reduces tricRNA levels. Although the integrity of this base pair is necessary for proper splicing, it is not sufficient. Furthermore, we found that strengthening weak base pairs in the pre-tRNA also impairs tricRNA production. We also used the reporters to identify *trans*-acting tricRNA processing factors. We found that several known tRNA processing factors, such as RtcB ligase and components of the TSEN endonuclease complex, are involved in tricRNA biogenesis. Depletion of these factors inhibits tRNA intron circularization. Furthermore, we observed that depletion of Clipper endonuclease results in increased tricRNA levels. In summary, our work characterizes the major players in *Drosophila* tricRNA biogenesis.

INTRODUCTION

Accurate processing of RNAs is crucial for their proper function *in vivo*; most primary transcripts can be considered as precursor molecules containing sequences that must be removed. One example of this phenomenon is in the transcription and processing of tRNA genes. As the translators between the languages of nucleic acids and polypeptides, tRNAs are essential for protein expression. Thus, it is important that they are processed correctly. In eukaryotes, transcription of pre-tRNAs is carried out by RNA polymerase III (1). Following transcription, a pre-tRNA molecule contains 5' leader and 3' trailer sequences, which are removed by RNase P and RNase Z, respectively (2, 3). In some instances, the

pre-tRNA transcript also contains an intron. Unlike messenger RNA splicing, which occurs by a large ribonucleoprotein complex called the spliceosome, tRNA splicing is carried out by a relatively small protein-only complex called TSEN (Figure 1). The pre-tRNA is first recognized by the TSEN (tRNA splicing endonuclease) complex, a heterotetramer consisting of two structural members, TSEN15 and TSEN54, and two catalytic members, TSEN2 and TSEN34 (4, 5). TSEN cleaves an intron-containing precursor into three segments: the 5' exon, an intron, and the 3' exon. Notably, this complex produces a 5'-OH and a 2',3'-cyclic phosphate at each site of cleavage.

Ligation of the exon halves is thought to be handled differently in different organisms (Figure 1). Plants and fungi utilize the “healing and sealing” pathway, wherein a multifunctional enzyme called Trl1 performs three distinct activities: a cyclic phosphodiesterase, to open the 2',3'-cyclic phosphate into a 3'-OH and 2'-phosphate; a kinase, to phosphorylate the 5'-OH of the intron and 3' exon; and a ligase, to join the exon halves together (Figure 1, top). A separate 2'-phosphotransferase enzyme called Tpt1 removes the remaining 2'-phosphate at the junction of the newly formed tRNA. The intron, now phosphorylated on its 5' end, is degraded by a 5' to 3' exonuclease, creating a supply of nucleotides (6).

In contrast, archaea and animals use the “direct ligation” pathway, wherein a ligase enzyme directly joins the exon halves together using the cyclic phosphate as the junction phosphate; there is no addition of an external phosphate onto the tRNA molecule (Figure 1, bottom). In archaea, the tRNA ligase is able to act on the intron ends to generate a circular RNA (7). Similarly, we have shown that RtcB, which ligates tRNA exon halves in *Drosophila*, also joins the intron ends together to make a circular RNA, which we term tRNA intronic circular (tric)RNA (8).

Although there have been many studies on the mechanism of pre-tRNA splicing in several organisms, much of this work comes from *in vitro* experiments, using purified proteins or cell extracts combined with an *in vitro* transcribed substrate. Thus, there is a need for an *in vivo* tRNA splicing model, where this processing pathway is placed in a cellular context. In this manuscript we present a unique system that allows us to detect both newly synthesized tRNAs and tricRNAs in *Drosophila* and human cultured cells. We take advantage of fluorescent RNA aptamer technology and northern blotting to elucidate the *cis*-acting elements and *trans*-acting factors necessary for proper tRNA and tricRNA biogenesis.

MATERIALS AND METHODS

Generation of reporter and mutant constructs

The human and *Drosophila* tricRNA reporters used in this study were made previously (9). To generate the dual reporter, four point mutations were introduced in the 3' exon of the *Drosophila* tricRNA reporter using Q5 Site-Directed Mutagenesis (NEB). For primer sequences, see Supplementary Table 1. Additional mutations within these three reporters were also generated using Q5 Site-Directed Mutagenesis (NEB). See Supplementary Table 1 for primer sequences.

Cell culture and transfections

For human cell culture, HEK293T cells were maintained in DMEM (Gibco) supplemented with 10% fetal bovine serum (HyClone) and 1% penicillin/streptomycin (Gibco) at 37° and 5% CO2. Cells (2 x 10^6) were plated in T25 flasks and transiently transfected with 2.5 µg plasmid DNA per flask using FuGENE HD transfection reagent (Promega) according to the manufacturer's protocol. Cells were harvested 72 hours post-transfection. RNA was isolated using TRIzol Reagent (Invitrogen), with a second chloroform extraction and ethanol rather than isopropanol precipitation (9).

For *Drosophila* cell culture, S2 cells were maintained in SF-900 serum-free medium (Gibco) supplemented with 1% penicillin-streptomycin and filter sterilized. Cells (5 x 10^6) were plated in T25 flasks and transiently transfected with 2.5 µg plasmid DNA per flask using Cellfectin II transfection reagent (Invitrogen) according to the manufacturer's protocol. Cells were harvested 72 hours post-transfection. RNA was isolated using TRIzol Reagent (Invitrogen), with a second chloroform extraction and ethanol rather than isopropanol precipitation (9). S2 RNAi was performed as described in (10) for 10 days, with dsRNA targeting Gaussia luciferase used as a negative control. In experiments with both RNAi and reporter expression, the reporter was transfected on day 7, and cells were harvested on day 10. Primers used to make PCR products for *in vitro* transcription can be found in Supplementary Table 1.

In-gel staining assay

RNA samples (5 µg) were electrophoresed through 10% TBE-urea gels (Invitrogen). Gels were washed 3X in dH_2O to allow renaturation of RNA and then incubated in DFHBI-1T staining solution (40 mM HEPES pH 7.4, 100 mM KCl, 1 mM $MgCl_2$, 10 µM DFHBI-1T (Lucerna)). Following staining, gels were imaged on an Amersham Typhoon 5. To visualize total RNA, gels were washed 3X in dH_2O, stained with ethidium bromide, and imaged on an Amersham Imager 600. Gels were quantified using ImageQuant TL software (GE Healthcare).

Northern blotting

RNA samples (5 µg) were separated by electrophoresis through 10% (for nuclease knockdown and overexpression experiments) or 15% (for dual reporter experiments) TBE-urea gels (Invitrogen). Following electrophoresis, the RNA was transferred to a nylon membrane (PerkinElmer). The membrane was dried overnight and UV-crosslinked. Pre-hybridization was carried out in Rapid-hyb Buffer (GE Healthcare) at 42°. Probes were generated by end-labeling oligonucleotides (IDT) with γ-^{32}P ATP (PerkinElmer) using T4 PNK (NEB), and then probes were purified using Illustra Microspin G-50 columns (GE Healthcare) to remove unincorporated nucleotides. Upon purification, probes were boiled, cooled on ice, and then added to the rapid-hyb buffer for hybridization. After hybridization, the membrane was washed in SSC buffer. For probe sequences, see Supplementary Table 1. Washing conditions are as follows. U1 and U6: hybridization at 65°, washes (twice in 2X SSC, twice in 0.33X SSC) at 60°. 7SK and dual reporter probe: hybridization at 42°, two washes in 5X SSC at 25°, and two washes in 1XSSC at 42°. For the dual reporter probe, two additional washes in 0.1XSSC at 45°

were performed. The membrane was then exposed to a storage phosphor screen (GE Healthcare) and imaged on an Amersham Typhoon 5.

RT-PCR

To test knockdown efficiency, total RNA was treated with TURBO DNase (Invitrogen) and then converted to cDNA using the SuperScript III kit (Invitrogen) with random hexamer priming. Primers for each candidate processing factor can be found in Supplementary Table 1.

Endonuclease overexpression cloning

To generate overexpression vectors, the Gateway system (Invitrogen) was used to clone ORFs of Dis3 and Clipper from S2 cell cDNA into either pAFW (*Drosophila* Genomics Resource Center, Barcode #1111) or pAWF (*Drosophila* Genomics Resource Center, Barcode #1112). Primers used to isolate Dis3 and Clipper can be found in Supplementary Table 1.

Western blotting

To test overexpression of candidate endonucleases, cells were washed in ice-cold 1X PBS and collected in ice-cold 1X PBS by scraping. The harvested cells were split into two portions: one for RNA isolation (see above) and one for protein isolation. Cells were pelleted by spinning at 2000 RPM for 5 minutes. The supernatant was removed and cells were lysed in ice-cold lysis buffer (50 mM Tris-HCl pH 7.5, 150 mM NaCl, 1 mM EDTA, 1% NP-40, 2X protease inhibitor cocktail (Invitrogen)) for 30 minutes on ice. The lysate was cleared by centrifugation at 13,000 RPM for 10 minutes at 4°. Protein lysate samples were electrophoresed through 4-12% Bis-Tris gels (Invitrogen). Following electrophoresis, protein lysate samples were transferred to a nitrocellulose membrane (GE Healthcare). The membrane was blocked in 5% milk in TBST. Washes and antibody dilutions were performed in TBST. The following antibodies and dilutions were used in this study: anti-FLAG M2 at 1:10,000 (Sigma) and anti-β-tubulin at 1:20,000 (Sigma). Membranes were imaged on an Amersham Imager 600.

Visualization of *Drosophila* BHB-like motifs

Sequences for all intron-containing pre-tRNAs were obtained from the genomic tRNA database (11, 12). The structure of the sequence containing the anticodon loop and intron was predicted using Mfold (13) and then drawn using VARNA (14).

RESULTS

Generation of *in vivo* splicing reporters

To characterize the *cis*-acting elements and *trans*-acting factors necessary for proper tricRNA splicing, we first sought to develop a reporter system that would allow us to detect newly synthesized tRNAs

and tricRNAs. Previously, we showed that human cells transfected with native fruit fly intronic tRNA genes readily express *Drosophila* tricRNAs (8). Moreover, when provided with either a human or fruit fly tRNA construct that contains a synthetic intron, human cells can also produce "designer" tricRNAs. For example, we inserted the 49nt Broccoli fluorescent RNA aptamer (15) into the introns of the human (TRYGTA3-1) and the *Drosophila* (CR31905) tRNA:Tyr_{GUA} genes (9). We term the resultant circular RNA "tricBroccoli," or tricBroc for short (16). This system is enhanced by use of external pol III promoters to increase overall expression levels (8, 9). A schematic of one such tricRNA reporter can be seen in Figure 2A, with the human U6* promoter. This reporter takes advantage of a 27nt sequence element within the U6 snRNA that promotes 5'-capping of the transcript (17), enhancing the stability of the linear precursor to facilitate downstream processing events (9). The human tricRNA reporter also contains a stretch of 11 base pairs situated between the tRNA domain and the Broccoli domain (Figure 2B, left). To determine the minimum length requirement for this fully-paired stem, we systematically deleted base pairs, and transfected the resulting constructs into HEK293T cells. We visualized expression of tricBroc using an in-gel fluorescence assay, where total RNA is run on a gel, soaked in a buffer containing the DFHBI fluorophore that binds to the Broccoli aptamer, and imaged using a laser scanner (8, 18) (Figure 2B, right). We found that reducing the stem below 7bp in length inhibited tricRNA formation, whereas stems of 8bp or greater yielded similar levels of tricBroc. Thus, we conclude that a stem of at least 8bp is necessary for proper splicing of the human tricRNA reporter. All subsequent experiments utilized a reporter with an 11bp stem.

To carry out studies in *Drosophila* cultured cells, we swapped the external human U6* promoter for the *Drosophila* one, including the first 27 nucleotides of the U6 snRNA (Figure 2A, "tricRNA reporter"; for additional details see (9)). This reporter was used as a base for the experiments in Figure 3. In order to detect both newly synthesized tricRNAs and tRNAs, we introduced four point mutations within the 3' exon of the tRNA that allow detection of mature reporter tRNAs by northern blotting (Figure 2A, "dual reporter"). To test expression of these constructs, we transfected the dual and the tricRNA reporters into S2 cells. We visualized tricRNA expression using the in-gel staining assay described above (Figure 2C, left panel). Although the tricRNA reporter expresses slightly higher levels of tricBroc, the dual reporter expresses appreciable levels. After staining for the Broccoli aptamer, the gel was re-stained with EtBr to detect total RNA (Figure 2C, middle panel). To determine if we could indeed detect newly synthesized tRNAs, we performed northern blotting with a radiolabeled oligoprobe specific for the dual reporter tRNA. The probe uniquely bound to the reporter tRNAs (Figure 2C right panel), indicating that it has sufficient specificity to differentiate between reporter and endogenous tRNAs. The tricRNA reporter was subsequently used for the experiments in Figure 3, whereas the dual reporter was utilized for those in Figure 5.

The helix portion of the BHB-like motif is important for proper processing

We next focused on the structural features of pre-tRNAs. In archaea, the pre-tRNA contains a structural motif known as a bulge-helix-bulge (BHB), which consists of a 4bp duplex flanked on each 3' end by a single-stranded 3nt bulge. This motif is both necessary and sufficient for splicing in archaea (19, 20). In contrast, eukaryotic splicing enzymes recognize the tRNA structure and although

a motif resembling a BHB is often present, the structural requirements for splicing do not seem to be as rigid (21, 22).The tricRNA reporters used in this study do not contain a canonical BHB, thus we refer to the structure as the "BHB-like motif" (Figure 3A). Due to its high degree of conservation among intron-containing tRNAs, we were interested in the first base pair of the helix, which we will refer to as the proximal base pair (PBP). Previous studies have referred to this base pair as the A-I (anticodon-intron) base pair, which is typically a pyrimidine-purine, respectively (23). In all 16 of the intronic tRNAs in *Drosophila*, this base pair is a C-G (Supplementary Figure S4). Thus, we wanted to determine the importance of the PBP for proper tRNA and tricRNA splicing. We generated a series of mutations in the tricRNA reporter and transfected the constructs into *Drosophila* S2 cells. To measure splicing efficiency, we performed an in-gel fluorescence assay on total RNA from the transfections (Figure 3B, left). We then normalized the intensities of the pre-tRNA and tricRNA bands using the 5S rRNA band from each lane, and expressed these values as a fraction of the total (Figure 3B, right). Interestingly, we observed that switching the base pair to a G-C had little effect; however, weakening it to an A-U or U-A reduced tricRNA levels. Further weakening the helix to a G-U or U-G yielded almost no product, and fully unpairing it (C-C) resulted in complete inhibition.

To determine if the mutations that disrupt production of the tricRNA also affect expression of the mature tRNA, we mutated the PBP in the dual reporter, allowing analysis of both newly synthesized tRNAs and tricRNAs (Supplementary Figure S1). As expected, unpairing the PBP affected production of both the tRNA and the tricRNA. On the basis of these results, we conclude that the strength, rather than the identity, of the PBP is important for efficient biogenesis of the reporter tRNA and tricRNA.

The pre-tRNA encoded by the tRNA:Tyr reporter construct is predicted to contain several weak (or perhaps non Watson-Crick) base pairs (Figure 3A, right). To determine if these weaker pairs are important, we first strengthened the helix by mutating the intronic bases (i.e. those on the 3' side of the stem). Introducing a single base pair at any position within this helix had little effect on splicing efficiency (Figure 3C, compare lane 1 to lanes 2-4). However, introducing two or three base pairs at a time reduced tricRNA production (lanes 5-7). The 5' side of the helix is located in exon 1 of the tRNA and the 3' side is part of the tricRNA; these halves must come apart in order to carry out exon ligation and intron circularization. Thus, we infer that if the helix is too tightly paired, splicing efficiency is reduced.

Mutations that are predicted to disrupt pairing within the BHB-like helix also inhibited formation of tricRNAs. We found that the integrity of the PBP alone is not sufficient for proper splicing; unpairing all of the other bases in the helix reduced tricRNA formation (Figure 3D, compare lanes 1 and 5). Similarly, fully unpairing the weak G•U pairs at positions 2 and 3 in the middle of the helix inhibited tricRNA production as well (lanes 3 and 4). However, introducing a single base pair adjacent to the proximal one in an otherwise unpaired helix partially rescued splicing (Figure 3D, lane 6). Interestingly, unpairing the distal base pair of the helix had no effect tricRNA splicing (Figure 3D, compare lanes 1 and 2). Because this helix base pair is furthest away from the proximal one, perhaps it may be less important for defining a specific structural motif. We conclude that a baseline level of pairing is required for optimal reporter tricRNA processing (see Discussion).

To elucidate whether these *cis*-element splicing determinants are applicable to other intron-containing pre-tRNAs, we developed a second reporter derived from *Drosophila* CR31143, an intron-containing tRNA:Leu_{CAA} gene (Supplementary Figure S2). Similar to our previous work with the tyrosine tricRNA reporter (9), we were able to increase tricRNA expression through use of the *Drosophila* snRNA:U6 and U6* external RNA polymerase III promoters (Supplementary Figure S2B). Although the BHB-like motif is slightly different than that of the tyrosine tricRNA reporter (Supplementary Figure S2A), we observed the same trends. Unpairing the PBP inhibited tricRNA production, and extending the helix by introducing A-U base pairs reduced tricRNA splicing (Supplementary Figure S2C). Interestingly, we noticed that tricBroc RNA from the leucine reporter presents as a doublet rather than as a single band (Supplementary Figures S2B, S2C). We also found that extending the helix affected migration of the doublet (Supplementary Figure S2C). To determine if the mutations affect splice site choice, we generated cDNA from these experiments and sequenced the tricRNA junctions (for details on this method, see (9)). We were surprised to find that tricRNAs from both wild-type and mutant leucine reporters each contained the same sequence at their splice junctions, despite the fact that they resolve as doublets and that the mutant RNAs migrate more slowly (Supplementary Figure S2D). This result suggests that the doublets are either topoisomers, or perhaps they contain differentially modified bases.

We were also curious to determine whether the *cis*-acting elements we identified in flies were also important for tRNA and tricRNA production in humans. Accordingly, we generated a series of mutations in the human tricRNA reporter (Figure 1A) and expressed these constructs in HEK293T cells (Supplementary Figure S2E). We found similar trends with the human reporter: pairing the helix to different degrees reduced reporter tricRNA formation, whereas unpairing the U-A base pair at position 4 had no effect. Furthermore, unpairing the PBP resulted in little to no tricRNA production. Taken together with the data in Figure 3, we conclude that similar rules govern tricRNA biogenesis in both vertebrates and invertebrates.

Pre-tRNA cleavage in *Drosophila* is carried out by orthologs of the TSEN complex

After characterizing *cis* elements important for proper tricRNA splicing, we next sought to identify tricRNA processing factors. We searched the database for *Drosophila* homologs of known human tRNA processing factors and found candidates for many of these genes (Figure 4A). To analyze these factors, we developed an RNA interference (RNAi) assay in S2 cells (Figure 4B). We investigated potential members of the tRNA splicing endonuclease complex (Figure 4A), which cleaves pre-tRNAs in both fungi (where it is called SEN) and humans (called TSEN) (24). Depletion of any member of this complex results in a dramatic reduction in both reporter tRNA and tricRNA formation (Figures 5A, 5B, and Supplementary Figure S3A). Concordantly, knockdown of TSEN proteins also results in accumulation of the pre-tRNA, visible as the top band in the Broccoli stained gel (Figure 5A). The pre-tRNA band can also be detected by northern blot, as the probe binds to a region in the 3'-exon (Figure 5B). From these data, we conclude that these genes indeed perform the functions of the TSEN complex in *Drosophila*.

Drosophila tRNA intron circularization proceeds through the direct ligation pathway

In archaea and eukarya, cleavage of an intron-containing pre-tRNA yields non-canonical RNA ends: a 5'-OH and a 2',3'-cyclic phosphate. Although plants and fungi use a roundabout “healing and sealing” approach, archaeal and animal cells are thought to utilize the direct ligation pathway, wherein there is no addition of an external phosphate (25). Previously, we showed that knockdown of CG9987 (now called RtcB) in *Drosophila* larvae and pupae resulted in a significant decrease in *tric31905* levels, along with a decrease in the corresponding tRNA:Tyr (8). However, this approach could not distinguish between newly transcribed and pre-existing RNAs and therefore likely underestimated the effect of RtcB depletion. Accordingly, we used the S2 cell RNAi system to assess levels of newly synthesized tRNAs and tricRNAs during RtcB knockdown. We also analyzed cells depleted of the other members of the human tRNA ligase complex, Archease and Ddx1 (Figure 4A). Depletion of RtcB caused a striking decrease in the tRNA and tricRNA reporters (Figures 5C, 5D, and Supplementary Figure S3B). Similarly, depletion of Archease and Ddx1 also resulted in reduction of both reporter RNAs. Importantly, depletion of the tRNA ligase complex did not cause accumulation of the pre-tRNA, reaffirming findings that cleavage and ligation are separable processes (26, 27). We conclude that RtcB is the *Drosophila* tRNA and tricRNA ligase, and that its activity is regulated by Archease and Ddx1.

tricRNA turnover is initiated by an endoribonuclease

Due to their lack of free 5' and 3' ends, circular RNAs exhibit a unique stability not afforded to their linear counterparts (8, 28, 29). Passive degradation of broken circles likely occurs via exonucleolytic decay, however active degradation of tricRNAs must be initiated by some type of endonuclease. To determine which enzymes are responsible for tricRNA turnover, we depleted S2 cells of candidate endoribonucleases, excluding those known to be directly involved in the RNAi pathway. We chose Zucchini, which is involved in piRNA biogenesis (30); Smg6, which is part of the nonsense-mediated mRNA decay pathway (31, 32); Dis3, a dual endo/exonuclease component of the nuclear exosome (33, 34); and Clipper, which has been shown to cleave RNA hairpins and is a homolog of mammalian CPSF 30K subunit (35, 36). Following knockdown (Figure 6C) and subsequent RNA isolation, we assessed endogenous tricRNA abundance by northern blotting for *tric31905*. As shown in Figure 6A and B, depletion of Zucchini, Smg6, or Dis3 had little to no effect on *tric31905* levels, whereas depletion of Clipper resulted in a modest increase in *tric31905*. We also performed a double knockdown of Dis3 and Clipper and observed a similar increase in *tric31905* levels (Figure 6A and B). In contrast, overexpression of FLAG-tagged Dis3 or Clipper did not reduce levels of *tric31905* (Figure 6D). Taken together, our data suggest that turnover of tric31905 is in part initiated by Clipper activity.

DISCUSSION

Removal of introns from pre-tRNAs is an essential step in their processing (24). Once thought to be discarded as waste products, we now know that metazoan tRNA introns are ligated into circular

RNAs in animals such as *D. melanogaster* and *C. elegans*. Here, we show that specific *cis*-acting elements are necessary for tRNA and tricRNA splicing, tricRNAs are produced by the tRNA splicing machinery in *Drosophila*, and tricRNA degradation is carried out by endonuclease activity.

Uncertainties regarding structure and stability

In archaea, intron-containing pre-tRNAs and pre-rRNAs are known to contain a highly conserved BHB motif (37). For many years, this motif was thought to be strictly required for proper splicing, although more recent work indicates that certain pre-tRNAs contain more relaxed BHB structures (38). We have found that *Drosophila* also display a wide variety of BHB-like motifs (Supplementary Figure S4). Perhaps the eukaryotic pre-tRNA structure is more relaxed in order to facilitate TSEN substrate interaction. Despite this diversity, we invariably identified a 3bp bulge at the 3' end of the helix (i.e. at the cut site between the intron and the 3' exon) (Supplementary Figure S4). Similarly, we consistently observed a constant number of bases between the 5' base of the PBP and the last base of the 5' exon (6nt, including the C in the PBP) (see Supplementary Figure S4). These regularities, combined with the lack of a strict BHB, suggest that *Drosophila* intron-containing pre-tRNAs are spliced in a manner akin to the molecular ruler mechanism outlined by others (21, 22). Due to an overall dearth of high-resolution data in eukaryotes, we can only speculate with regard to the structure of the substrate-bound form of the metazoan TSEN complex.

Although we can draw broad conclusions from the various helix pairing and unpairing experiments, we cannot know for sure if these mutations cause alternative pre-tRNA structures to form. Similarly, we do not know if these mutations affect pre-tRNA stability. For example, unpairing the BHB helix may cause destabilization of the entire pre-tRNA, leading to its degradation (Figure 3D, see pre-tRNA band). This result is in contrast to the experiments in Figure 3B and C, where there is a clear accumulation of the pre-tRNA in several mutant constructs. Perhaps this accumulation is due to structural changes. Mutations to the PBP could disrupt the invariant 3bp bulge and reduce recognition of the intron-3' exon cut site. Similarly, if the helix region is too tightly paired, the rigidity of the duplex may interfere with positioning of the cut sites or otherwise reduce interaction with the TSEN complex. In the future, high-resolution (e.g. NMR) structure-function analysis of wild-type and mutant BHB-like motifs could shed light on these issues.

Fungi and metazoa: distinct intron fates

Two pathways for tRNA ligation exist in nature: the “healing and sealing” pathway, utilized by plants and fungi, and the “direct ligation” pathway, found in archaea and animals (24). Plants and fungi lack RtcB-family enzymes and thus only have one way to ligate tRNA exons (39, 40). Similarly, archaea do not possess healing and sealing enzymes and therefore can only join RNA ends by direct ligation (25). Although metazoans appear to primarily use the direct ligation pathway (25), there is evidence for healing and sealing-type splicing in higher organisms. For example, mammalian genomes contain an RNA polynucleotide kinase (CLP1) and a 2',3'-cyclic nucleotide phosphodiesterase (CNP) that can perform the corresponding activities of yeast Trl1 (41, 42); they also contain a putative 2'-phosphotransferase called TRPT1 (43). Additionally, a Trl1-like tRNA ligase activity has been

detected in human cells (44). However, mouse *Cnp1* and *Trpt1* are not essential, as a knockouts of either of these genes does not affect organismal viability (45, 46). Thus, a yeast-like tRNA splicing pathway may exist in mammals, but it likely contributes little to overall tRNA production. In this study, we have shown that direct ligation is the primary tRNA and tricRNA biogenesis pathway used in flies. Similar to the situation in mammals, we cannot exclude a role for the *Drosophila* healing and sealing pathway in developmental regulation or in response to cellular stress. Perhaps this alternative pathway might be utilized in a tissue-specific or stress-induced manner. As evidence, the fruit fly genome contains homologs of TRPT1 and CLP1. Additional studies will be needed to assess the overall contribution of these genes to the regulation of tRNA and tricRNA expression in *Drosophila*.

It is interesting to consider why *Drosophila* tRNA introns are circularized, rather than being immediately degraded, as is their typical fate in yeast (6). One possibility is that tricRNAs serve an important function, and so production of these circRNAs would outweigh the energetic benefits of creating a supply of free nucleotides. Previously, we observed a high degree of conservation of *tric31905* among the twelve fully-sequenced Drosophilid species (8). In particular, there is significant co-variation within the predicted *tric31905* secondary structure, suggesting that there has been selection for a specific structure over evolutionary time (8). Consistent with these observations, we previously identified reads from small RNA-seq datasets that map to the intron of *CR31905* (8). Taken together with Figure 6, it seems likely that Clipper is involved in the observed downstream processing of *tric31905* into 21nt fragments (8). Whether these downstream processing events lead to formation of RNA silencing complexes has yet to be determined. Alternatively, endonucleolytic cleavage by Clipper might initiate the process of tricRNA degradation. Given that Clipper exhibits a preference for binding RNAs with G- and/or C-rich regions (36), it is also possible that different endonucleases may cleave different tricRNAs.

Irrespective of the ultimate fate or function of metazoan tRNA introns, these observations raise an important evolutionary question. As mentioned above, the genomes of plants and fungi do not contain RtcB homologs and their tRNA introns are typically linear (6, 47). In contrast, archaeal and metazoan genomes contain *RtcB* and they express tricRNAs (7, 8). Is RtcB the determining factor for tRNA intron circularization? One prediction of this hypothesis is that loss of the healing and sealing pathway and complementation via the direct ligation pathway (Figure 1) should not only rescue tRNA biogenesis but also result in tricRNA formation. Accordingly, Shuman and colleagues have shown that bacterial *RtcB* can complement deletion of yeast *Trl1*, which is an essential gene (48). More recently, analysis of tRNA introns isolated from this *RtcB* replacement strain shows that they are, as predicted, circularized (A. Bao and A. Hopper, personal communication).

These data suggest that intron circularization may be a normal “byproduct” of RtcB exon ligation. RtcB is the eponymous member of an RNA ligase family that requires a 5'-OH and a 2',3'-cyclic phosphate in order to carry out its enzymatic activity (27). Because these atypical RNA termini are generated by RNase L type endonucleases, a second prediction is that mRNA exons that are ligated by RtcB would also generate circular introns. Indeed, recent work strongly supports this idea. IRE1 is an RNase L family endonuclease that cleaves *HAC1* mRNA during the unfolded protein response in yeast (49) and *XBP1* mRNA in metazoan cells (50). The long-sought RNA ligase responsible for

catalyzing this unconventional RNA splicing event during the metazoan UPR is RtcB (51–53). In budding yeast, Trl1 ligates the two *HAC1* exons and the linear intron is degraded. However, in the *Trl1Δ,RtcB* replacement yeast strain, the *HAC1* intron was also recently shown to be circularized (BioRxiv: https://doi.org/10.1101/452516). These findings provide strong support for the notion that fungal tRNA introns are primarily linear because yeast lack RtcB.

Implications for human disease

An interesting aspect of the tRNA splicing pathway is that mutations in human tRNA processing factors have been shown to cause neurological disease. For example, there are several clinical reports of mutations in nearly any member of the human TSEN complex that lead to pontocerebellar hypoplasia (54–60). Furthermore, homozygous mutation of the *CLP1* kinase gene in consanguineous Turkish families causes similar phenotypes (61, 62). Animal models of *TSEN54* (63) and *CLP1* (61, 62, 64) function exhibit decreases in viability, longevity, and locomotion; reduced brain size due to apoptosis was also observed in these models. The extent to which these defects are linked to tRNA processing is unknown.

In humans, tRNA introns are simply too small (~16-20nt) to be included in typical RNA-seq cDNA libraries. Similarly, human tricRNAs would not be enriched within miRNA or siRNA libraries because they are circular and do not contain ends that are needed for library adaptor ligation. However, human cells readily generate tricRNAs bearing various reporter introns (8, 9, 16). Thus it seems highly probable that endogenous tricRNAs are regulated features of human transcriptomes. However, even if endogenous tricRNAs do not perform essential functions on their own, they may serve as biomarkers for therapeutic agents aimed at restoring tRNA processing defects in human patients. Future studies will require genetically facile animal models in order to test the direct contribution of tRNA and tricRNA processing to neurological disease progression.

ACKNOWLEDGEMENT

The authors thank Steve Rogers for assistance with S2 cells and Anita Hopper for communicating unpublished results.

FUNDING

This work was supported by a grant (to A.G.M.) from the National Institutes of Health, R01-GM118636. C.A.S. was supported in part by a National Science Foundation Graduate Research Fellowship, DGE-1650116, and by a Dissertation Completion fellowship from the University of North Carolina Graduate School. Funding for open access charge: National Institute of General Medical Sciences.

CONFLICT OF INTEREST

The authors declare no conflict of interest.

REFERENCES

1. Phizicky,E.M. and Hopper,A.K. (2010) tRNA biology charges to the front. *Genes Dev.*, **24**, 1832–60.
2. Walker,S.C. and Engelke,D.R. (2006) Ribonuclease P: The evolution of an ancient RNA enzyme. *Crit. Rev. Biochem. Mol. Biol.*, **41**, 77–102.
3. Vogel,A., Schilling,O., Späth,B. and Marchfelder,A. (2005) The tRNase Z family of proteins: Physiological functions, substrate specificity and structural properties. *Biol. Chem.*, **386**, 1253–1264.
4. Paushkin,S., Patel,M., Furia,B., Peltz,S. and Trotta,C. (2004) Identification of a human endonuclease complex reveals a link between tRNA splicing and pre-mRNA 3′ end formation. *Cell*, **117**, 311–321.
5. Trotta,C.R., Miao,F., Arn,E.A., Stevens,S.W., Ho,C.K., Rauhut,R. and Abelson,J.N. (1997) The Yeast tRNA Splicing Endonuclease: A Tetrameric Enzyme with Two Active Site Subunits Homologous to the Archaeal tRNA Endonucleases. *Cell*, **89**, 849–858.
6. Wu,J. and Hopper,A.K. (2014) Healing for destruction: TRNA intron degradation in yeast is a two-step cytoplasmic process catalyzed by tRNA ligase Rlg1 and 5′-to-3′ exonuclease Xrn1. *Genes Dev.*, **28**, 1556–1561.
7. Salgia,S., Singh,S., Gurha,P. and Gupta,R. (2003) Two reactions of Haloferax volcanii RNA splicing enzymes: Joining of exons and circularization of introns. *RNA*, **9**, 319–330.
8. Lu,Z., Filonov,G.S., Noto,J.J., Schmidt,C.A., Hatkevich,T.L., Wen,Y., Jaffrey,S.R. and Gregory Matera,A. (2015) Metazoan tRNA introns generate stable circular RNAs in vivo. *RNA*, **21**, 1554–1565.
9. Schmidt,C.A., Noto,J.J., Filonov,G.S. and Matera,A.G. (2016) A Method for Expressing and Imaging Abundant, Stable, Circular RNAs in Vivo Using tRNA Splicing. *Methods Enzymol.*, **572**, 215–236.
10. Rogers,S.L. and Rogers,G.C. (2008) Culture of Drosophila S2 cells and their use for RNAi-mediated loss-of-function studies and immunofluorescence microscopy. *Nat. Protoc.*, **3**, 606–611.
11. Chan,P.P. and Lowe,T.M. (2009) GtRNAdb: A database of transfer RNA genes detected in genomic sequence. *Nucleic Acids Res.*, **37**, 93–97.
12. Chan,P.P. and Lowe,T.M. (2016) GtRNAdb 2.0: An expanded database of transfer RNA genes identified in complete and draft genomes. *Nucleic Acids Res.*, **44**, D184–D189.
13. Zuker,M. (2003) Mfold web server for nucleic acid folding and hybridization prediction. *Nucleic Acids Res.*, **31**, 3406–3415.
14. Darty,K., Denise,A. and Ponty,Y. (2009) VARNA: Interactive drawing and editing of the RNA secondary structure. *Bioinformatics*, **25**, 1974–1975.

15. Filonov,G.S., Moon,J.D., Svensen,N. and Jaffrey,S.R. (2014) Broccoli: Rapid selection of an RNA mimic of green fluorescent protein by fluorescence-based selection and directed evolution. *J. Am. Chem. Soc.*, **136**, 16299–16308.
16. Noto,J.J., Schmidt,C.A. and Matera,A.G. (2017) Engineering and expressing circular RNAs via tRNA splicing. *RNA Biol.*, **14**, 978–984.
17. Good,P.D., Krikos,A.J., Li,S.X.L., Bertrand,E., Lee,N.S., Giver,L., Ellington,A., Zaia,J.A., Rossi,J.J. and Engelke,D.R. (1997) Expression of small, therapeutic RNAs in human cell nuclei. *Gene Ther.*, **4**, 45–54.
18. Filonov,G.S., Kam,C.W., Song,W. and Jaffrey,S.R. (2015) In-Gel Imaging of RNA Processing Using Broccoli Reveals Optimal Aptamer Expression Strategies. *Chem. Biol.*, **22**, 649–660.
19. Thompson,L.D. and Daniels,J. (1988) A tRNA(Trp) intron endonuclease from Halobacterium volcanii. Unique substrate recognition properties. *J. Biol. Chem.*, **263**, 17951–17959.
20. Thompson,L.D. and Daniels,C.J. (1990) Recognition of exon-intron boundaries by the Halobacterium volcanii tRNA intron endonuclease. *J. Biol. Chem.*, **265**, 18104–18111.
21. Greer,C., Söll,D. and Willis,I. (1987) Substrate recognition and identification of splice sites by the tRNA-splicing endonuclease and ligase from Saccharomyces cerevisiae. *Mol. Cell. Biol.*, **7**.
22. Reyes,V.M. and Abelson,J. (1988) Substrate recognition and splice site determination in yeast tRNA splicing. *Cell*, **55**, 719–730.
23. Baldi,M.I., Mattoccia,E., Bufardeci,E., Fabbri,S. and Tocchini-Valentini,G.P. (1992) Participation of the intron in the reaction catalyzed by the Xenopus tRNA splicing endonuclease. *Science*, **255**, 1404–1408.
24. Yoshihisa,T. (2014) Handling tRNA introns, archaeal way and eukaryotic way. *Front. Genet.*, **5**, 1–16.
25. Popow,J., Schleiffer,A. and Martinez,J. (2012) Diversity and roles of (t)RNA ligases. *Cell. Mol. Life Sci.*, **69**, 2657–70.
26. Peebles,C.L., Ogden,R.C., Knapp,G. and Abelson,J. (1979) Splicing of yeast tRNA precursors: a Two-Stage Reaction. *Cell*, **18**, 27–35.
27. Popow,J., Englert,M., Weitzer,S., Schleiffer,A., Mierzwa,B., Mechtler,K., Trowitzsch,S., Will,C.L., Lührmann,R., Söll,D., *et al.* (2011) HSPC117 is the essential subunit of a human tRNA splicing ligase complex. *Science*, **331**, 760–4.
28. Wilusz,J.E. (2017) Circular RNAs: Unexpected outputs of many protein-coding genes. *RNA Biol.*, **14**, 1007–1017.
29. Holdt,L.M., Kohlmaier,A. and Teupser,D. (2018) Molecular roles and function of circular RNAs in eukaryotic cells. *Cell. Mol. Life Sci.*, **75**, 1071–1098.
30. Nishimasu,H., Ishizu,H., Saito,K., Fukuhara,S., Kamatani,M.K., Bonnefond,L., Matsumoto,N., Nishizawa,T., Nakanaga,K., Aoki,J., *et al.* (2012) Structure and function of Zucchini endoribonuclease in piRNA biogenesis. *Nature*, **491**, 284–287.
31. Gatfield,D., Unterholzner,L., Ciccarelli,F.D., Bork,P. and Izaurralde,E. (2003) Nonsense-mediated mRNA decay in Drosophila: At the intersection of the yeast and mammalian pathways. *EMBO J.*, **22**, 3960–3970.

32. Glavan,F., Behm-Ansmant,I., Izaurralde,E. and Conti,E. (2006) Structures of the PIN domains of SMG6 and SMG5 reveal a nuclease within the mRNA surveillance complex. *EMBO J.*, **25**, 5117–5125.
33. Cairrão,F., Arraiano,C. and Newbury,S. (2005) Drosophila gene tazman, an orthologue of the yeast exosome component Rrp44p/Dis3, is differentially expressed during development. *Dev. Dyn.*, **232**, 733–737.
34. Mamolen,M. and Andrulis,E.D. (2009) Characterization of the Drosophila melanogaster Dis3 ribonuclease. *Biochem. Biophys. Res. Commun.*, **390**, 529–534.
35. Bai,C. and Tolias,P.P. (1996) Cleavage of RNA hairpins mediated by a developmentally regulated CCCH zinc finger protein. *Mol. Cell. Biol.*, **16**, 6661–6667.
36. Bai,C. and Tolias,P.P. (1998) Drosophila clipper/CPSF 30K is a post-transcriptionally regulated nuclear protein that binds RNA containing GC clusters. *Nucleic Acids Res.*, **26**, 1597–1604.
37. Lykke-Andersen,J., Aagaard,C., Semionenkov,M. and Garrett,R.A. (1997) Archaeal introns: splicing, intercellular mobility and evolution. *Trends Biochem. …*, **22**, 326-.
38. Marck,C. and Grosjean,H. (2003) Identification of BHB splicing motifs in intron-containing tRNAs from 18 archaea: evolutionary implications. *Rna*, **9**, 1516–1531.
39. Englert,M. and Beier,H. (2005) Plant tRNA ligases are multifunctional enzymes that have diverged in sequence and substrate specificity from RNA ligases of other phylogenetic origins. *Nucleic Acids Res.*, **33**, 388–99.
40. Wang,L.K., Schwer,B., Englert,M., Beier,H. and Shuman,S. (2006) Structure-function analysis of the kinase-CPD domain of yeast tRNA ligase (Trl1) and requirements for complementation of tRNA splicing by a plant Trl1 homolog. *Nucleic Acids Res.*, **34**, 517–527.
41. Ramirez,A., Shuman,S. and Schwer,B. (2008) Human RNA 5'-kinase (hClp1) can function as a tRNA splicing enzyme in vivo. *RNA*, **14**, 1737–45.
42. Schwer,B., Aronova,A., Ramirez,A., Braun,P. and Shuman,S. (2008) Mammalian 2',3' cyclic nucleotide phosphodiesterase (CNP) can function as a tRNA splicing enzyme in vivo. *RNA*, **14**, 204–210.
43. Spinelli,S.L., Malik,H.S., Consaul,S.A. and Phizicky,E.M. (1998) A functional homolog of a yeast tRNA splicing enzyme is conserved in higher eukaryotes and in Escherichia coli. *Proc. Natl. Acad. Sci. U. S. A.*, **95**, 14136–14141.
44. Zillmann,M., Gorovsky,M.A. and Phizicky,E.M. (1991) Conserved mechanism of tRNA splicing in eukaryotes. *Mol. Cell. …*, **11**.
45. Lappe-Siefke,C., Goebbels,S., Gravel,M., Nicksch,E., Lee,J., Braun,P.E., Griffiths,I.R. and Navel,K.A. (2003) Disruption of Cnp1 uncouples oligodendroglial functions in axonal support and myelination. *Nat. Genet.*, **33**, 366–374.
46. Harding,H.P., Lackey,J.G., Hsu,H.C., Zhang,Y., Deng,J., Xu,R.M., Damha,M.J. and Ron,D. (2008) An intact unfolded protein response in Trpt1 knockout mice reveals phylogenic divergence in pathways for RNA ligation. *RNA*, **14**, 225–232.
47. Knapp,G., Ogden,R.C., Peebles,C.L. and Abelson,J. (1979) Splicing of yeast tRNA precursors: structure of the reaction intermediates. *Cell*, **18**, 37–45.

48. Tanaka,N., Meineke,B. and Shuman,S. (2011) RtcB, a novel RNA ligase, can catalyze tRNA splicing and HAC1 mRNA splicing in vivo. *J. Biol. Chem.*, **286**, 30253–30257.
49. Sidrauski,C. and Walter,P. (1997) The transmembrane kinase Ire1p is a site-specific endonuclease that initiates mRNA splicing in the unfolded protein response. *Cell*, **90**, 1031–1039.
50. Yoshida,H., Matsui,T., Yamamoto,A., Okada,T. and Mori,K. (2001) XBP1 mRNA is induced by ATF6 and spliced by IRE1 in response to ER stress to produce a highly active transcription factor. *Cell*, **107**, 881–891.
51. Lu,Y., Liang,F.X. and Wang,X. (2014) A Synthetic Biology Approach Identifies the Mammalian UPR RNA Ligase RtcB. *Mol. Cell*, **55**, 758–770.
52. Kosmaczewski,S.G., Edwards,T.J., Han,S.M., Eckwahl,M.J., Meyer,B.I., Peach,S., Hesselberth,J.R., Wolin,S.L. and Hammarlund,M. (2014) The RtcB RNA ligase is an essential component of the metazoan unfolded protein response. *EMBO Rep.*, **15**, 1278–1286.
53. Ray,A., Zhang,S., Rentas,C., Caldwell,K.A. and Caldwell,G.A. (2014) RTCB-1 Mediates Neuroprotection via XBP-1 mRNA Splicing in the Unfolded Protein Response Pathway. *J. Neurosci.*, **34**, 16076–16085.
54. Budde,B.S., Namavar,Y., Barth,P.G., Poll-The,B.T., Nürnberg,G., Becker,C., van Ruissen,F., Weterman,M. a J., Fluiter,K., te Beek,E.T., *et al.* (2008) tRNA splicing endonuclease mutations cause pontocerebellar hypoplasia. *Nat. Genet.*, **40**, 1113–1118.
55. Cassandrini,D., Biancheri,R., Tessa,A., Di Rocco,M., Di Capua,M., Bruno,C., Denora,P., Sartori,S., Rossi,A., Nozza,P., *et al.* (2010) Pontocerebellar hypoplasia. *Neurology*, **75**, 1459–1464.
56. Namavar,Y., Chitayat,D., Barth,P.G., van Ruissen,F., de Wissel,M.B., Poll-The,B.T., Silver,R. and Baas,F. (2011) TSEN54 mutations cause pontocerebellar hypoplasia type 5. *Eur. J. Hum. Genet.*, **19**, 724–6.
57. Namavar,Y., Barth,P.G., Kasher,P.R., van Ruissen,F., Brockmann,K., Bernert,G., Writzl,K., Ventura,K., Cheng,E.Y., Ferriero,D.M., *et al.* (2011) Clinical, neuroradiological and genetic findings in pontocerebellar hypoplasia. *Brain*, **134**, 143–56.
58. Valayannopoulos,V., Michot,C., Rodriguez,D., Hubert,L., Saillour,Y., Labrune,P., de Laveaucoupet,J., Brunelle,F., Amiel,J., Lyonnet,S., *et al.* (2012) Mutations of TSEN and CASK genes are prevalent in pontocerebellar hypoplasias type 2 and 4. *Brain*, **135**, 1–5.
59. Battini,R., D'Arrigo,S., Cassandrini,D., Guzzetta,A., Fiorillo,C., Pantaleoni,C., Romano,A., Alfei,E., Cioni,G. and Santorelli,F.M. (2014) Novel mutations in TSEN54 in pontocerebellar hypoplasia type 2. *J. Child Neurol.*, **29**, 520–5.
60. Breuss,M.W., Sultan,T., James,K.N., Rosti,R.O., Scott,E., Musaev,D., Furia,B., Reis,A., Sticht,H., Al-Owain,M., *et al.* (2016) Autosomal-Recessive Mutations in the tRNA Splicing Endonuclease Subunit TSEN15 Cause Pontocerebellar Hypoplasia and Progressive Microcephaly. *Am. J. Hum. Genet.*, **99**, 228–235.
61. Schaffer,A.E., Eggens,V.R.C., Caglayan,A.O., Reuter,M.S., Scott,E., Coufal,N.G., Silhavy,J.L., Xue,Y., Kayserili,H., Yasuno,K., *et al.* (2014) CLP1 founder mutation links tRNA splicing and maturation to cerebellar development and neurodegeneration. *Cell*, **157**, 651–63.

62. Karaca,E., Weitzer,S., Pehlivan,D., Shiraishi,H., Gogakos,T., Hanada,T., Jhangiani,S.N., Wiszniewski,W., Withers,M., Campbell,I.M., *et al.* (2014) Human CLP1 mutations alter tRNA biogenesis, affecting both peripheral and central nervous system function. *Cell*, **157**, 636–50.
63. Kasher,P.R., Namavar,Y., van Tijn,P., Fluiter,K., Sizarov,A., Kamermans,M., Grierson,A.J., Zivkovic,D. and Baas,F. (2011) Impairment of the tRNA-splicing endonuclease subunit 54 (tsen54) gene causes neurological abnormalities and larval death in zebrafish models of pontocerebellar hypoplasia. *Hum. Mol. Genet.*, **20**, 1574–84.
64. Hanada,T., Weitzer,S., Mair,B., Bernreuther,C., Wainger,B.J., Ichida,J., Hanada,R., Orthofer,M., Cronin,S.J., Komnenovic,V., *et al.* (2013) CLP1 links tRNA metabolism to progressive motor-neuron loss. *Nature*, **495**, 474–80.

TABLE AND FIGURE LEGENDS

Figure 1: tRNA splicing pathway. Pre-tRNAs are transcribed by RNA polymerase III and contain a 5' leader and 3' trailer sequence. A structural motif resembling the archaeal bulge-helix-bulge (BHB) is present in the pre-tRNA. The leader and trailer are removed by ribozymes. Cleavage of the pre-tRNA yields two exon halves and an intron, each bearing 5'-OH and 2',3'-cyclic phosphate at the cut sites. In plants and fungi, a multifunctional enzyme phosphorylates the 5' end of both the 3' exon and intron, opens the cyclic phosphodiesterase, and ligates the exon halves to make a mature tRNA. A separate 2'-phosphotransferase removes the extra phosphate (“healing and sealing”). The intron is degraded by an exonuclease. In archaea and animals, a single enzyme joins both the exon halves and the intron ends to yield a mature tRNA and a circular RNA (“direct ligation”).

Figure 2: Developing a reporter. (A) Schematic of reporter constructs used in this study. Each contains either the human or *Drosophila* external U6 snRNA promoter as well as the first 27 nucleotides of U6 snRNA (denoted as U6*). The reporters also contain a *Drosophila* tyrosine tRNA (purple) with the Broccoli fluorescent RNA aptamer as a synthetic intron (green). The “dual reporter” contains four point mutations in the 3' exon that allow specific detection by a Northern blot probe. (B) A stem of at least 8 base pairs is necessary for proper splicing of the human tricRNA reporter. Left: Schematic of the human tricRNA reporter pre-tRNA, showing a variable stem length region. Right: In-gel fluorescence assay showing optimal stem length for the reporter. The 5S rRNA band from the total RNA gel was used as a loading control. (C) The dual reporter produces tricRNAs detectable by DFHBI stain and tRNAs detectable by Northern blot. Left: DFHBI- and EtBr-stained gels showing expression of the dual and tricRNA reporters. The entire EtBr-stained gel is shown as a loading control rather than just the 5S rRNA band. Right: Northern blot of the dual and tricRNA reporters. 7SK is shown as a loading control.

Figure 3: The helix portion of the BHB-like motif is important for proper tricRNA splicing. (A) Left: Schematic of the tricRNA reporter pre-tRNA, with emphasis of the BHB-like motif. Right: Nucleotide sequence of the BHB-like motif in the tricRNA reporter. The proximal base pair (PBP) is outlined in blue. The other base pairs of the helix are numbered 1-4. The darker bases are part of the tRNA, and the lighter bases are part of the intron. (B) Alterations to the PBP disrupt tricRNA splicing. Left: In-gel

fluorescence assay of mutations to the PBP. Each lane represents a different identity of the PBP. The 5S rRNA band from the EtBr-stained gel is shown as a loading control. Right: quantification of three biological replicates. The pre-tRNA and tricRNA bands were each normalized to the 5S band, and averages of those values were expressed as a fraction of the total. (C) Pairing the helix reduces tricRNA formation. Left: In-gel fluorescence assay of constructs pairing the helix. Each lane represents base pairs being introduced at various positions in the helix (see number positioning in panel A). The 5S rRNA band from the EtBr-stained gel is shown as a loading control. Right: quantification of three biological replicates. Quantifications were carried out as above. (D) Unpairing the helix inhibits tricRNA production. Left: In-gel fluorescence assay of constructs unparing the helix. Each lane represents bases being paired or unpaired at various positions in the helix (see number positioning in panel A). The 5S rRNA band from the EtBr-stained gel is shown as a loading control. Right: quantification of three biological replicates. Quantifications were carried out as above.

Figure 4: Experimental setup for trans factor experiments. (A) Table of human tRNA processing factors and *Drosophila* sequence homologs. (B) Schematic of S2 cell RNAi assay. Candidate processing factors were knocked down for 10 days by adding dsRNA to the media daily. At day 7, the dual reporter was transfected. At day 10, cells were harvested for RNA analysis.

Figure 5: tricRNA and tRNA biogenesis in S2 cells proceeds through the direct ligation pathway. (A) Knocking down any member of the TSEN complex inhibits reporter tricRNA production. In-gel fluorescence assay of RNA from S2 cells depleted of TSEN complex members. The pre-tRNA and tricRNA bands are identified. The 5S rRNA band from the EtBr-stained gel is shown as a loading control. For knockdown efficiency, see Supplementary Figure S3A. (B) Knocking down various members of the TSEN complex also reduces reporter tRNA formation. Northern blot of RNA from S2 cells depleted of TSEN complex members using a probe specific to the dual reporter. The pre-tRNA and tRNA bands are identified. U1 snRNA is used as a loading control. For knockdown efficiency, see Supplementary Figure S3A. (C) Knocking down RtcB ligase or its associated factors Archease and Ddx1 inhibits reporter tricRNA production. In-gel fluorescence assay of RNA from S2 cells depleted of RtcB, Archease, or Ddx1. The pre-tRNA and tricRNA bands are identified. The 5S rRNA band from the EtBr-stained gel is shown as a loading control. For knockdown efficiency, see Supplementary Figure S3B. (D) Knocking down RtcB, Archease, or Ddx1 also reduces reporter tRNA formation. Northern blot of RNA from S2 cells depleted of RtcB, Archease, or Ddx1 using a probe specific to the dual reporter. The pre-tRNA and tRNA bands are identified. U1 snRNA is used as a loading control. For knockdown efficiency, see Supplementary Figure S3B.

Figure 6: Clipper endonuclease is required for tricRNA turnover. (A) Northern blot of RNA from endonuclease-depleted S2 cells. U1 and U6 snRNA are shown as loading controls. (B) Quantification of three biological replicates. The tric31905 bands were normalized to U6 snRNA bands and average values were plotted. Error bars denote standard error of the mean. (C) RT-PCR for candidate endonucleases to test knockdown efficiency in S2 cells. RT-PCR for 5S rRNA was used as a control. (D) Western blot showing overexpression of candidate endonucleases. S2 cells were transfected with FLAG-tagged endonuclease constructs. Cells from each condition were split in half for both RNA and

protein isolation. The top two panels are a Northern blot of RNA from the experiment, and the bottom two panels are a Western blot of protein lysate from the experiment. For the Northern, U6 snRNA is used as a loading control; for the Western, tubulin is used as a loading control.

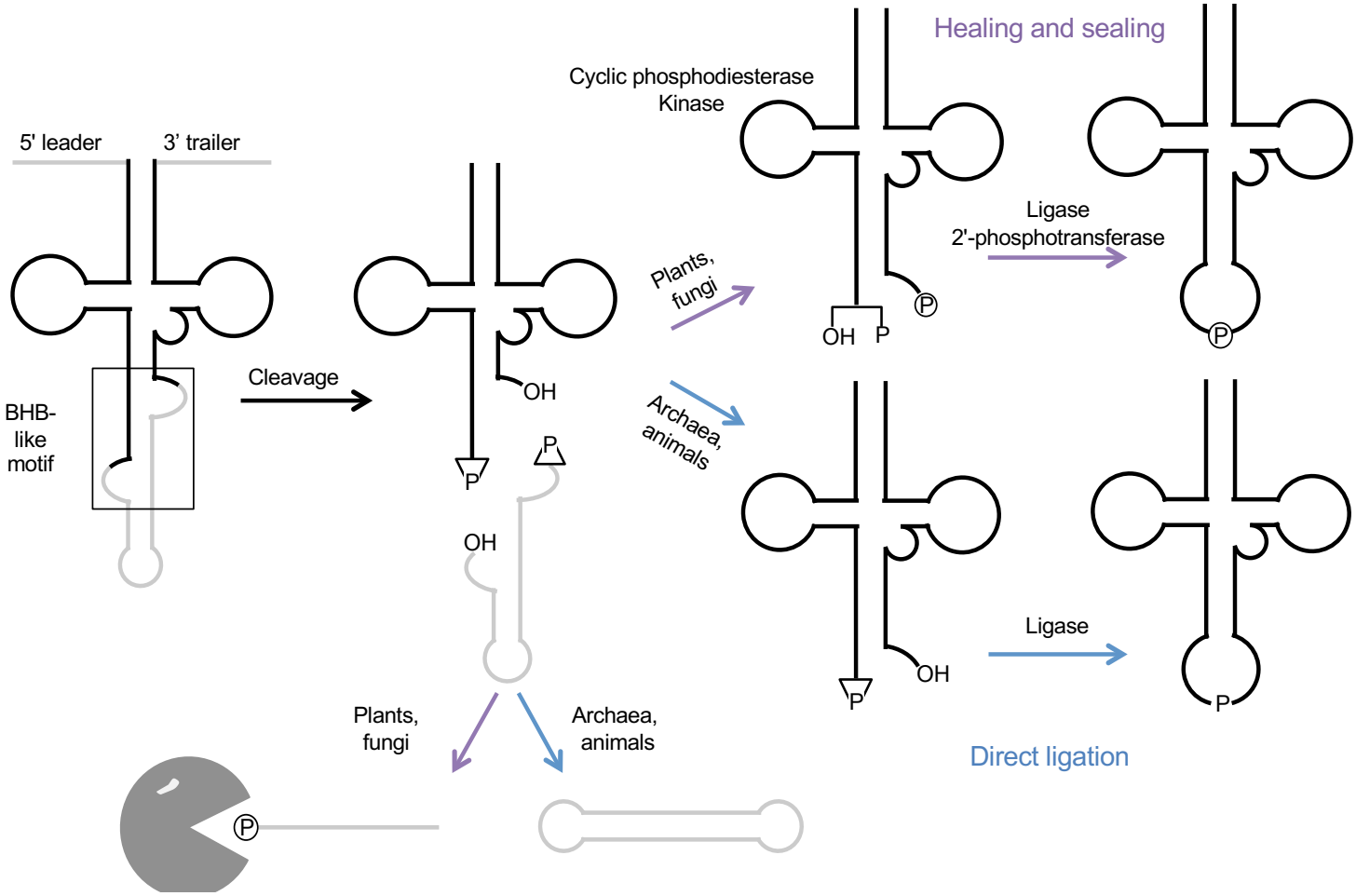
Healing and sealing
Cyclic phosphodiesterase
Kinase
5' leader
3' trailer
Ligase
2'-phosphotransferase
Plants,
fungi
BHB-
like
motif
Cleavage
OH
P
OH
P
Archaea,
animals
OH
P
Ligase
OH
P
P
Plants,
fungi
Archaea,
animals
Direct ligation
P

Figure 1

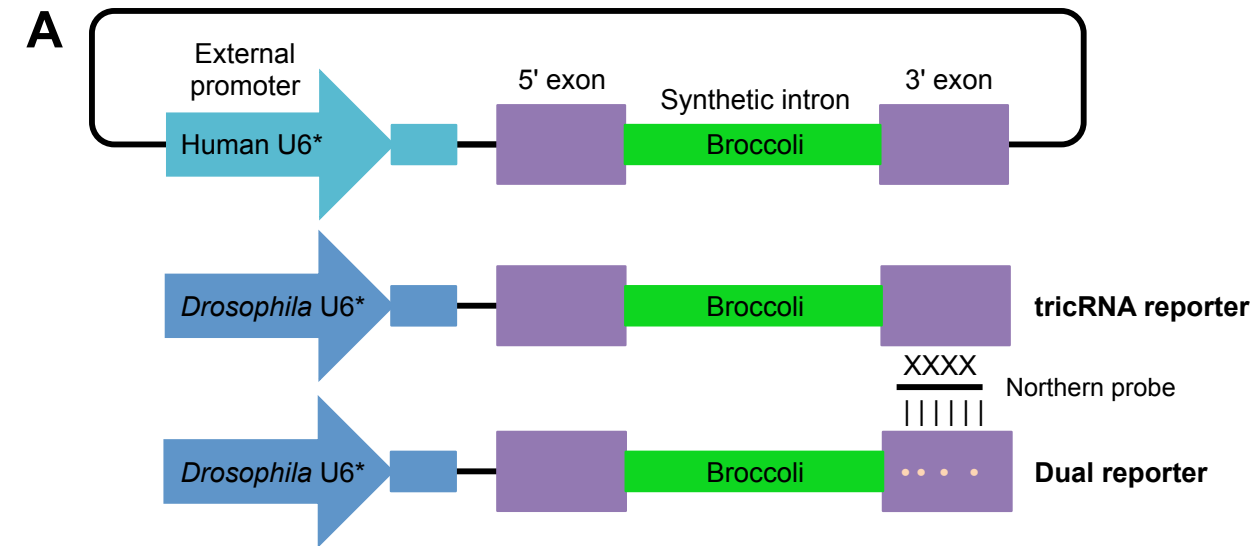
A
External promoter
Human U6*
5' exon
Synthetic intron
Broccoli
3' exon
Drosophila U6*
Broccoli
tricRNA reporter
XXXX
Northern probe
Drosophila U6*
Broccoli
Dual reporter

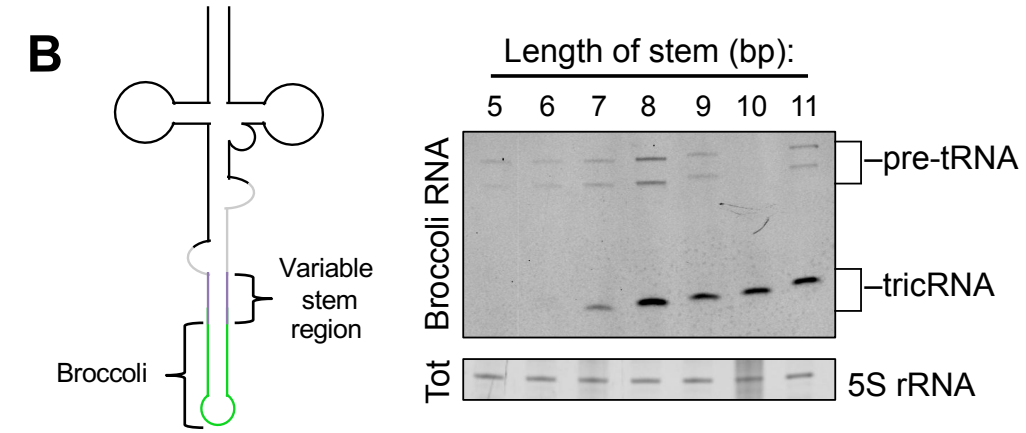
B
Variable stem region
Broccoli
Length of stem (bp):
5 6 7 8 9 10 11
Broccoli RNA
–pre-tRNA
–tricRNA
Tot
5S rRNA

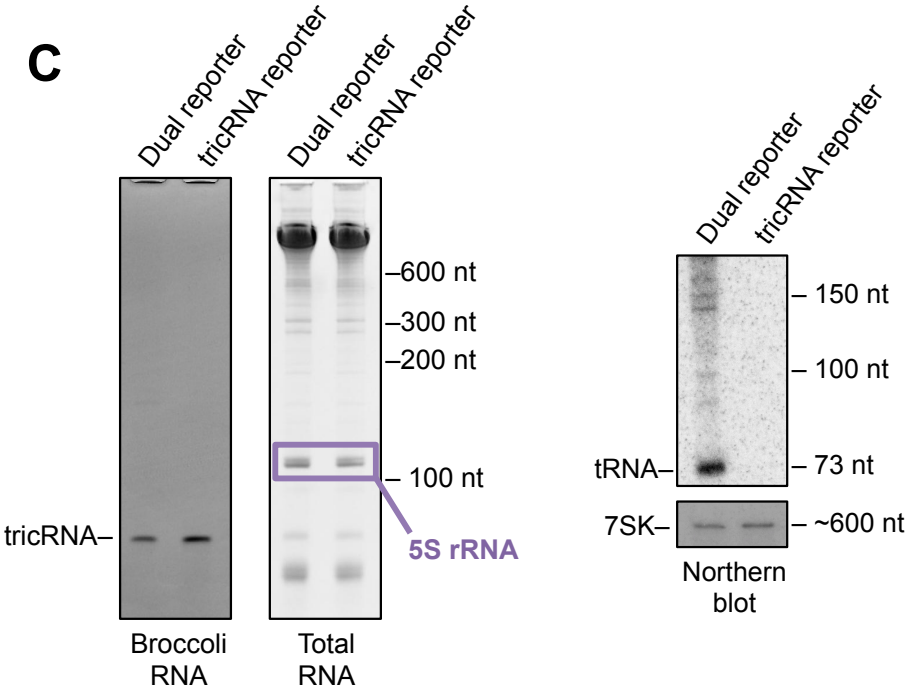
C
Dual reporter
tricRNA reporter
Dual reporter
tricRNA reporter
–600 nt
–300 nt
–200 nt
– 100 nt
tricRNA–
5S rRNA
Broccoli RNA
Total RNA
Dual reporter
tricRNA reporter
– 150 nt
– 100 nt
tRNA–
– 73 nt
7SK–
– ~600 nt
Northern blot

Figure 2

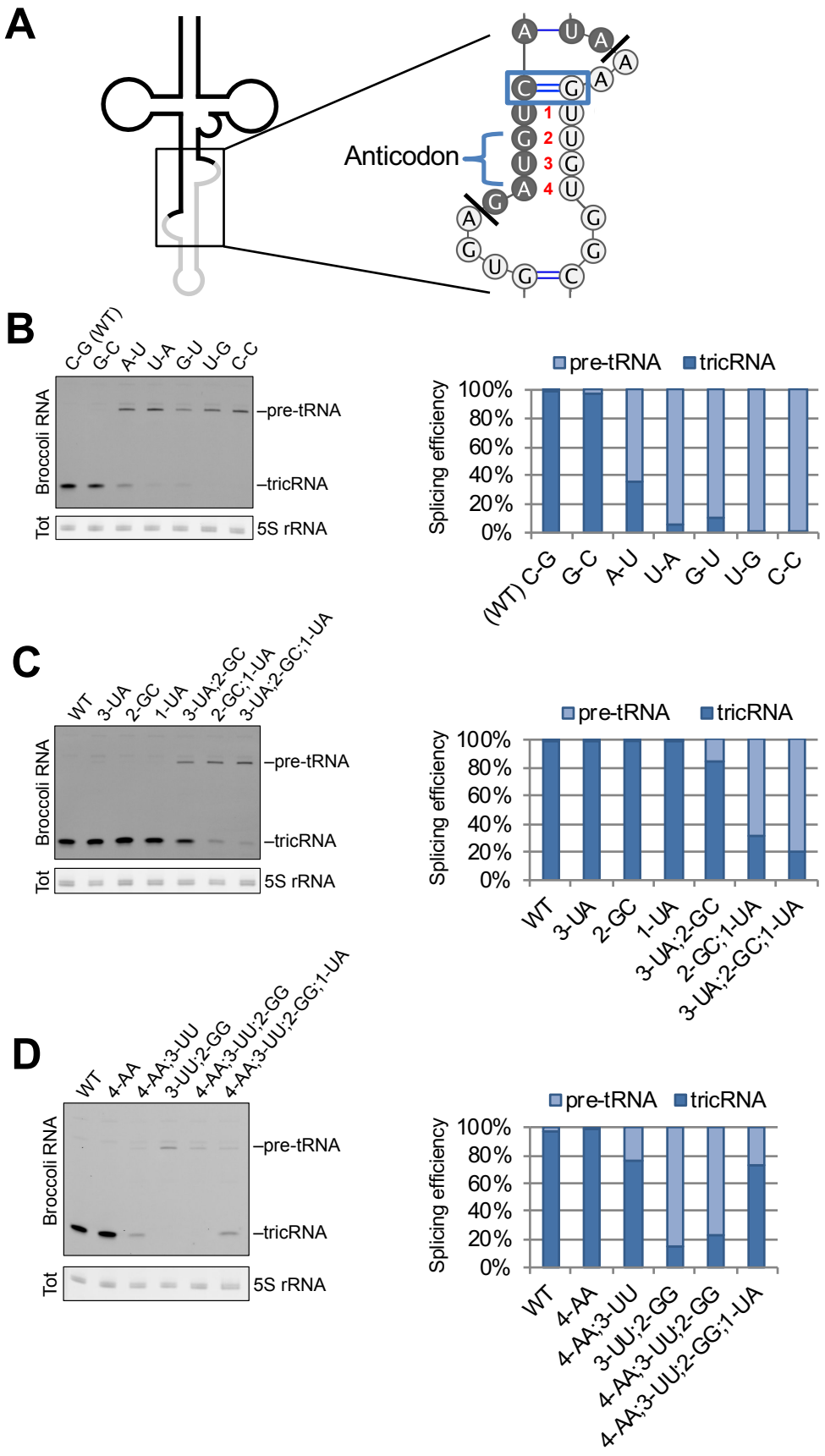
A
Anticodon
B
C-G (WT)
G-C
A-U
U-A
G-U
U-G
C-C
Broccoli RNA
–pre-tRNA
–tricRNA
Tot
5S rRNA
pre-tRNA
tricRNA
Splicing efficiency
100%
80%
60%
40%
20%
0%
(WT) C-G
G-C
A-U
U-A
G-U
U-G
C-C
C
WT
3-UA
2-GC
1-UA
3-UA;2-GC
2-GC;1-UA
3-UA;2-GC;1-UA
D
WT
4-AA
4-AA;3-UU
3-UU;2-GG
4-AA;3-UU;2-GG
4-AA;3-UU;2-GG;1-UA

Figure 3

A

	Human	Fly
tRNA Splicing Endonuclease	TSEN54	CG5626
	TSEN34	CG33260
	TSEN15	CG30343
	TSEN2	CG31812
Ligase	RTCB	RtcB
	DDX1	Ddx1
	ZBTB8OS	Archease

B

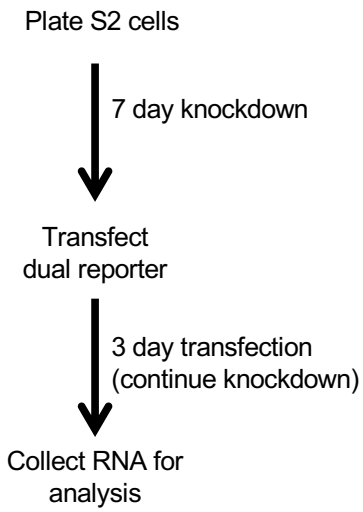

Figure 4

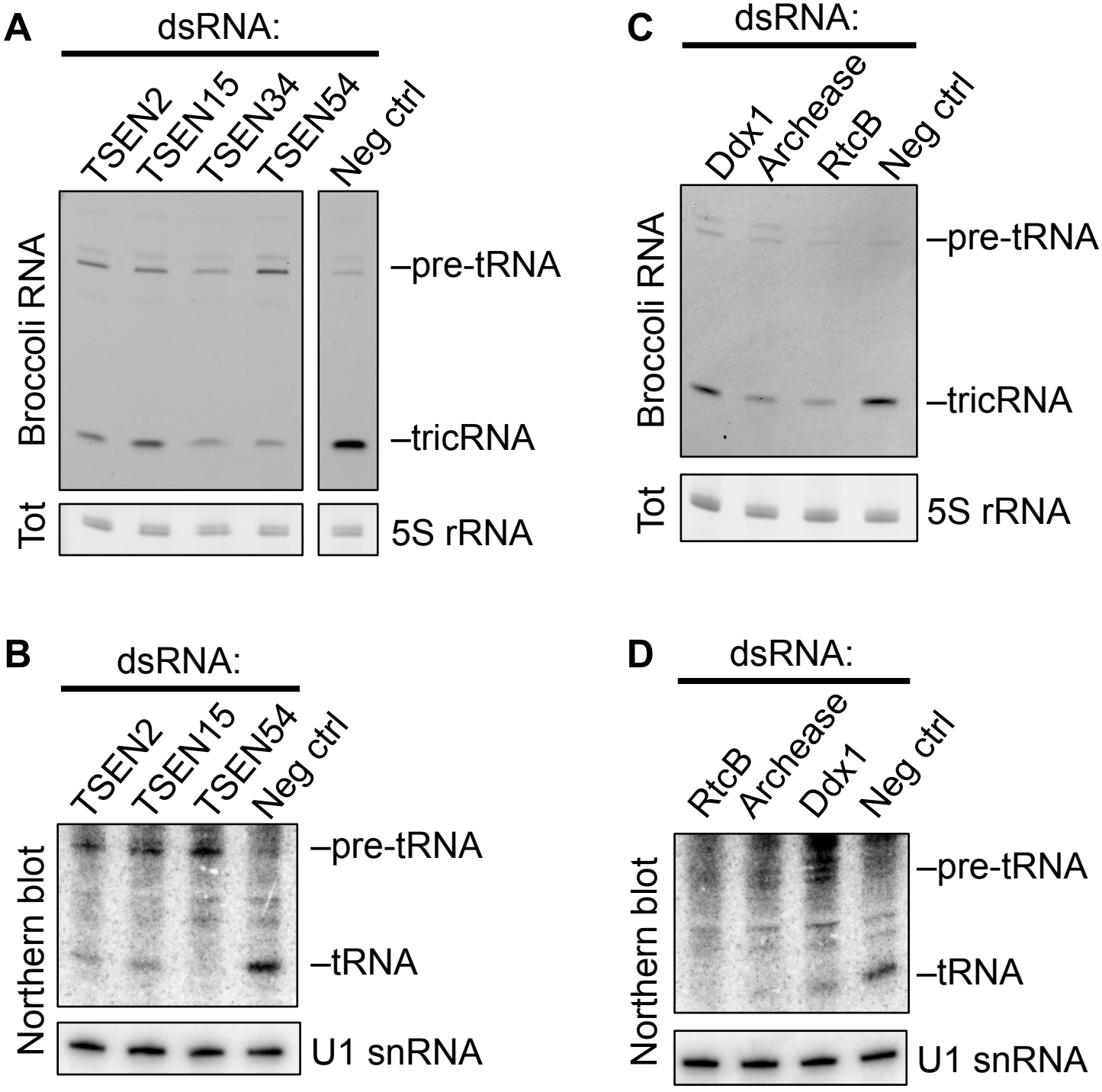
A
dsRNA:
TSEN2
TSEN15
TSEN34
TSEN54
Neg ctrl
Broccoli RNA
–pre-tRNA
–tricRNA
Tot
5S rRNA
C
dsRNA:
Ddx1
Archease
RtcB
Neg ctrl
Broccoli RNA
–pre-tRNA
–tricRNA
Tot
5S rRNA
B
dsRNA:
TSEN2
TSEN15
TSEN54
Neg ctrl
Northern blot
–pre-tRNA
–tRNA
U1 snRNA
D
dsRNA:
RtcB
Archease
Ddx1
Neg ctrl
Northern blot
–pre-tRNA
–tRNA
U1 snRNA

Figure 5

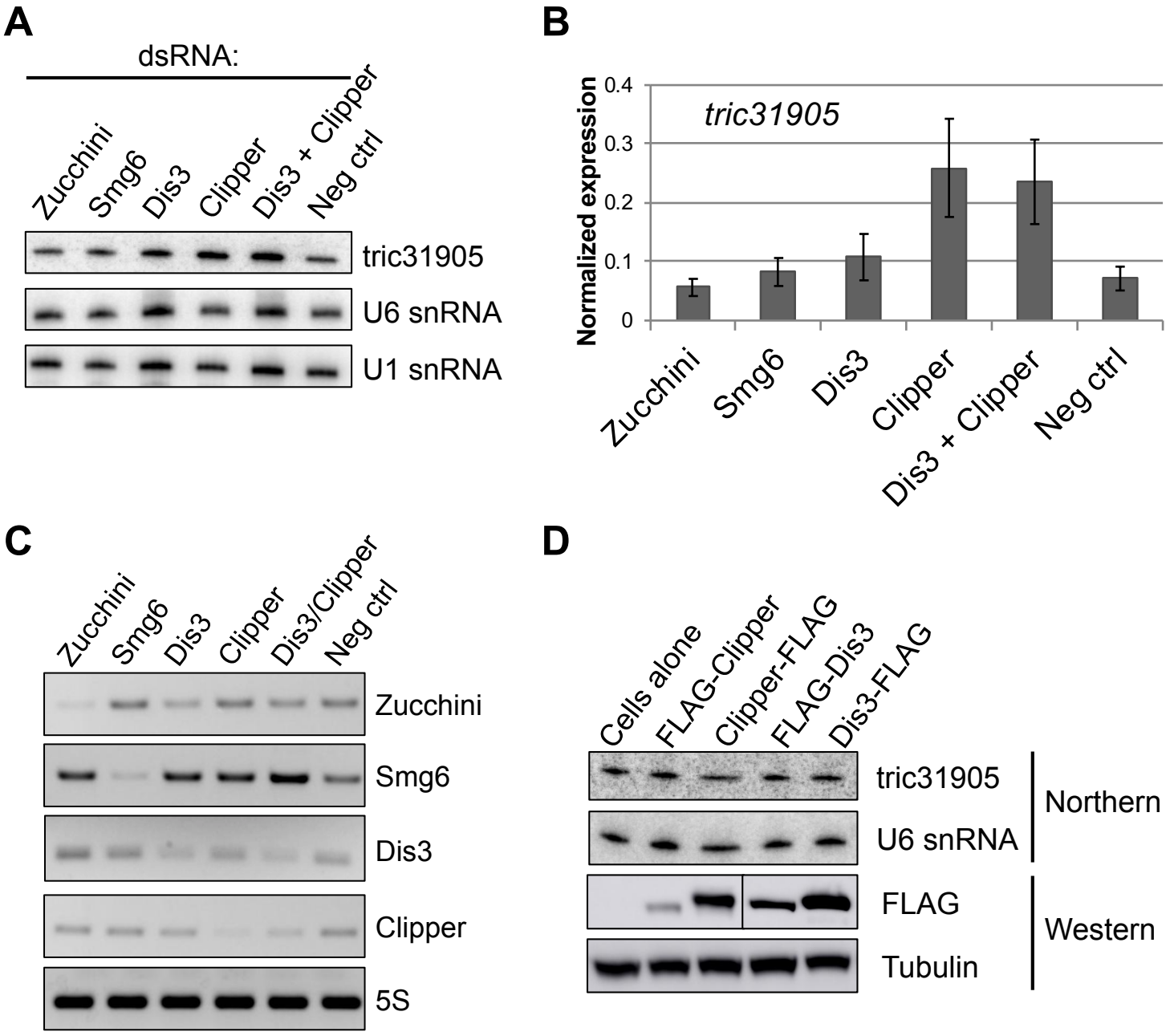
A
dsRNA:
Zucchini
Smg6
Dis3
Clipper
Dis3 + Clipper
Neg ctrl
tric31905
U6 snRNA
U1 snRNA
B
tric31905
Normalized expression
0.4
0.3
0.2
0.1
0
Zucchini
Smg6
Dis3
Clipper
Dis3 + Clipper
Neg ctrl
C
Zucchini
Smg6
Dis3
Clipper
Dis3/Clipper
Neg ctrl
Zucchini
Smg6
Dis3
Clipper
5S
D
Cells alone
FLAG-Clipper
Clipper-FLAG
FLAG-Dis3
Dis3-FLAG
tric31905
U6 snRNA
FLAG
Tubulin
Northern
Western

Figure 6